Available online at www.easdprocedia.org
EASD Procedia EURODYN (2020) 3251-3260

EASD Procedia

EURODYN 2020
XI International Conference on Structural Dynamics
M. Papadrakakis, M. Fragiadakis, C. Papadimitriou (eds.)
Athens, Greece, 23–26 November 2020

PERFORMANCE OF A LINEAR SOLUTION FOR APPROXIMATING NONLINEAR RESPONSE OF REINFORCED CONCRETE STRUCTURES SUBJECTED TO EARTHQUAKE SHAKING

Kevin Kariuki[1], Tarjei Heen[1], Lars Halvor Kaasa[1], and Amir M. Kaynia [2,3]

[1]Dr. Ing. A. Aas-Jakobsen
Lilleakerveien 4a, 0283 Oslo, Norway
e-mail: {kka,the,lhk}@aaj.no

[2] Department of Structural Engineering, Norwegian University of Science and Technology, Richard Birkelandsvei 1a, 7491 Trondheim, Norway
e-mail: amir.kaynia@ntnu.no

[3] Norwegian Geotechnical Institute, P.O- Box 3930 Ullevaal Stadion, 0806 Oslo, Norway
e-mail: amir.m.kaynia@ngi.no

Keywords: Seismic analysis, Nonlinear analysis, Suspension bridges, Concrete pylons.

Abstract. *Nonlinear Time History Analyses (NTHA) are generally regarded as the most accurate way of predicting the dynamic response of a structure to a given seismic ground motion. However, these types of analyses are computationally demanding and require proper software. The aim of this paper is to investigate the feasibility and accuracy of an Equivalent Linear analysis (ELA) where material nonlinearity is accounted for through an iterative procedure with the use of secant stiffnesses. The method is applied to one of the pylons of a major suspension bridge recently designed in Chile. For comparative purposes, two models are created in the open-source framework OpenSees: 1) a full nonlinear fiber model where nonlinear material behaviour is accounted for through distributed plasticity, and 2) an elastic model where the element flexural stiffnesses are updated using the ELA method. The analyses are carried out for seven earthquake time histories. The results show that the ELA is able to reproduce the maximum forces in the structure with a satisfactory accuracy. However, the method is not able to capture regaining of stiffness once cracks are closed due to cyclic responses.*
For further verification, several pushover analyses are also conducted on both models with the inertial forces extracted from the most unfavourable time-steps in the nonlinear time domain analysis. The pushover analysis verifies that the ELA method is capable of predicting the structural response up to the point of yielding of the steel reinforcement or crushing of the concrete. Nevertheless, the method is fairly accurate in identifying possible plastic hinges, and to some degree, assessing the ductility of the structure.

ISSN:2311-9020
Peer-review under responsibility of the Organizing Committee of EURODYN 2020.
doi: 10.47964/1120.9266.19338

1 INTRODUCTION

Large suspension bridges are particularly susceptible to earthquake excitation due to their slender configurations. When built in seismic active areas, earthquake induced forces often become the most prominent design criteria, thus accurately capturing this effect during design calculations are of top priority. This is no exception for the Chacao Bridge, which upon completion will connect the island of Chiloé to the Chilean mainland. The suspension bridge spans approximately 2750 meters, divided into two main spans of 1155 and 1055 meters supported by three pylons. The Norwegian consultant company Aas-Jakobsen participated in the international design team tasked with designing the bridge. One of the firm's task was design of the bridge pylons. The northern and southern pylons consist of two pylon legs connected by three girders, all of which are made from hollow Reinforced Concrete (RC) sections. With the bridge located in one of the most seismic active regions in the world, namely the subduction zone between the Nazca Plate and the South American Plate [1, 2], a complete time history analysis (THA) was deemed necessary to predict the structures response to a seismic event. The analysis was carried out in RM-Bridge [3] with seven ground motion records corresponding to a seismic event with a return period of 1030-years (Maximum Probable Earthquake) [4].

Although widely recognised as an accurate way of capturing the behaviour of structures subjected to cyclic dynamic forces [5], running a full NTHA on large structures such as the Chacao Bridge quickly becomes a momentous task and convergence is not guaranteed. If, however, the sections of the structure are expected to exceed their elastic domain during an seismic event, the forces resulting from an THA may be too conservative since the ductile behaviour of the structure is not captured [6].

To cope with the issue of overestimating forces when designing the Chacao Bridge pylons, an iterative procedure was proposed, hereby referred to as the ELA. First, the nonlinear moment-curvature relation was calculated for each section in the Finite Element (FE) model. Then, a series of elastic THAs was carried out using the same ground motion record. Following each analysis, the largest absolutes moment for each section was obtained and used together with the appropriate moment curvature relation to determine the secant stiffness of that section. A new elastic model with updated stiffness properties was then established. When the flexural stiffnesses of the sections converge after a number of THAs, the nonlinear material response of the structure is considered approximately captured. The final iteration with converged stiffness properties will therefore in principal have the same resulting forces as those following a full NTHA. An elastic analysis with secant stiffnesses is allowed by the AASHTO Seismic Design Manual, as long as the distribution of forces are verified to be consistent with expected nonlinear behaviour [7]. The use of cracked stiffness properties is also recommended by the Eurocode 8 when performing a linear elastic analyses [8]. However, it appears that little attention has been paid to investigate the consistency between the two methods. A comparative study was therefore conducted using the South Pylon of the Chacao Bridge. A FE model with linear elastic elements was developed in OpenSees [9], onto which the ELA could be conducted. A second model with nonlinear material properties was used as a baseline. Finally, multiple pushover analyses were performed for further verification of the methods capabilities.

2 MODEL DESCRIPTION

2.1 OpenSees Model

The FE model of the South Pylon in this study was established in the open source software framework OpenSees [9]. The geometry and material properties of the models were based on

the RM-Bridge model previously created by Aas-Jakobsen during the design of the Chacao Bridge with minor modifications. The suspension cables were simplified as springs at the top of each pylon leg. Additionally, the foundation SSI-matrices were simplified by neglecting off-diagonal terms and modelling the remaining parts as linear springs.
For the comparative purpose of this study, two models were established; a model with nonlinear material properties using the fiber section functionality provided in OpenSees and a linear elastic model. The nonlinear fiber model utilized the built-in material models *Concrete02* [10] and *Steel02* [11] for the concrete and reinforcement fibers, respectively. The moment-curvature relations used in the ELA were obtained with the same material models. The chosen material parameters are summarized in Tables 1 and 2.

Parameter	Symbol	Value
Expected maximum compressive strength	f_{pc}	58.5 MPa
Initial modulus of elasticity	E_{cm}	32.1 GPa
Strain at maximum compressive strength	ε_{c0}	3.64 ‰
Ultimate compressive strength	f_{pcu}	49 MPa
Ultimate compressive strain	ε_{cu}	5 ‰
Expected tensile strength	f_t	4.05 MPa
Tensile softening stiffness	E_{ts}	4.41 MPa
Ratio between unloading and initial slope	λ	0.5

Table 1: *Concrete02* material parameters.

Parameter	Symbol	Value
Expected yield strength	f_y	470 MPa
Young's modulus	E_s	200 GPa
Yield strain	ε_y	2.35 ‰
Strain hardening ratio	b	0.06
Isotropic hardening parameter	a_1	0
Isotropic hardening parameter	a_2	1
Isotropic hardening parameter	a_3	0
Isotropic hardening parameter	a_4	1
Asymptote parameter	R_0	0.20
Asymptote parameter	cR_1	0.925
Asymptote parameter	cR_2	0.15

Table 2: *Steel02* material parameters.

P-Δ transformation was applied in order to capture nonlinear geometry effects, with the pylon carrying gravity loads from the bridge deck in addition to its self weight resulting in severe compression forces. Damping was included as Rayleigh damping, with a chosen target damping ratio of 5 % for the two fundamental modes in the longitudinal and transverse directions of the bridge.

2.2 Model verification

As the discretization of the fiber section is important for the performance of both the full nonlinear analysis and the ELA method, a study on discretization was conducted to decide on the appropriate average size of the concrete fibers in the pylon. The study was performed by calculating the moment-curvature diagrams for representative sections along the pylon with varying axial forces. The results revealed that a mesh consisting of 25×10 concrete fibers per side of each pylon leg element was sufficiently accurate without restricting the efficiency of the analyses, as seen in Figure 1.

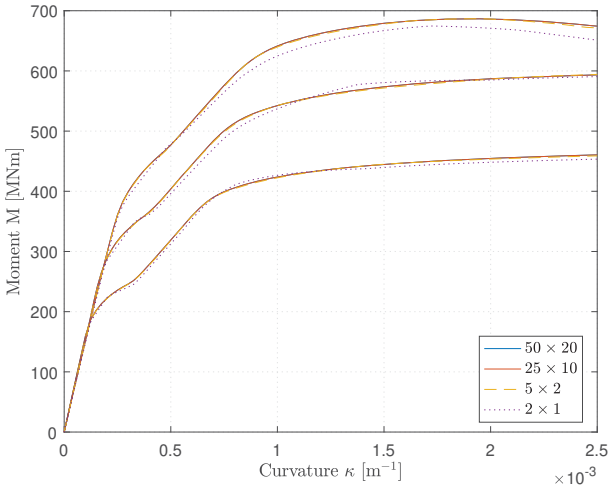

Figure 1: Moment-curvature relations for different meshing and axial load.

The modal properties of the two models were compared to verify that their initial stiffnesses and therefore initial dynamic properties would be similar. The mean deviation of modal periods for the first 20 modes is 1.26%, with a maximum deviation of 2.15% in mode number 20. This was deemed sufficiently accurate to assume similar initial behaviour between the models under both static and dynamic loading.

3 ANALYSIS PROCEDURE

3.1 Equivalent Linear Analysis

The algorithm for the ELA was developed using a combination of the THA solver in OpenSees and MATLAB for post-processing data. The method is largely based on nonlinear moment-curvature relations for the RC sections, so these are initially computed by performing a section response analysis for each fiber section in OpenSees. Since this relation depends on axial force, seen in Figure 2a, a series of different scaling of the gravity load was applied so that each element had a number of moment-curvature diagrams associated with it. The stiffness properties of the initial linear elastic elements were taken as the slope of the tangent at the origin for the corresponding moment-curvature relations with unit gravity load. A full transient THA was then conducted in OpenSees using the the linear elastic model and Newmark's constant average acceleration method as time-stepping scheme. The selected ground motion was applied in both horizontal directions with a time step of 0.01 seconds. Data regarding forces, acceleration and displacements was recorded during the analysis and upon completion written to text files. MATLAB was then invoked to post process the results. For each element, MATLAB scripts obtained the maximum moment about both principle axes along with the corresponding axial forces. The

updated stiffness about each axis was then obtained by finding the intersection point between the moment and the appropriate moment-curvature relation, as shown in Figure 2b. By making use of the relation

$$EI = \frac{M}{\kappa} \tag{1}$$

where M and κ is the moment and curvature about the section axis, the secant stiffness was taken as the slope of a line going through the origin and the intersection point. Since the axial load changes for each iteration during the procedure, the intersection point was linearly interpolated between existing curves, enveloping moment-curvature relations so to avoid recomputing these for each iteration.

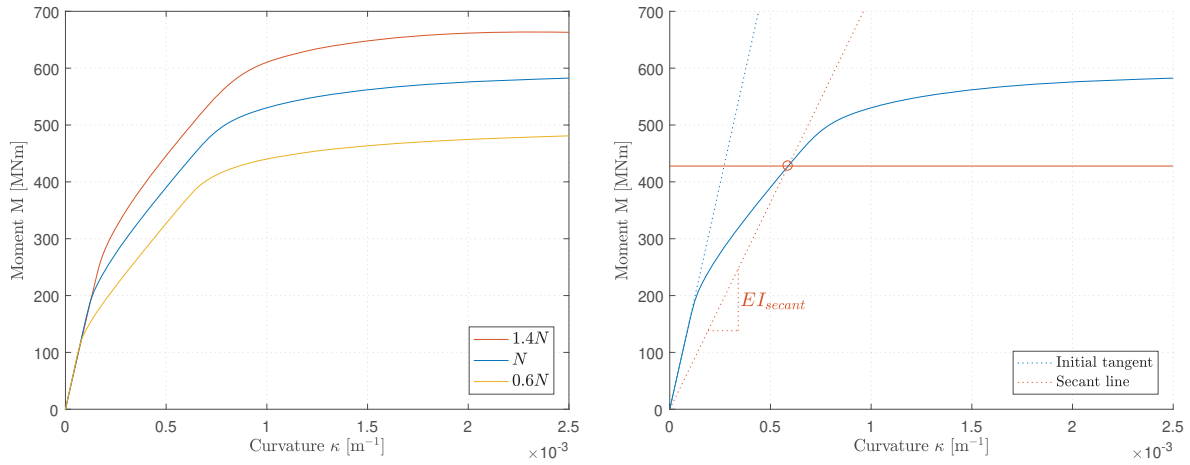

(a) Effect of compressive load for M-κ relation.

(b) Secant line in M-κ relation.

Figure 2: Determination of secant line using moment.

The updated stiffness for each element was taken as the mean between the newly acquired and previous value, to ensure smoothness during the scheme. A new linear elastic model with updated stiffness properties was then created. If the newly obtained stiffness values differed significantly from the previous ones, another iteration was initiated using the updated model. The iterations continue until the change in all element stiffnesses falls below a given convergence threshold.

3.2 Pushover Analysis

The pushover analyses were conducted with inertial forces as basis for the load distribution. For each critical element, e.g. base elements in the pylon legs or cross-beams, the total acceleration in each node was retrieved for the time-step where the maximum bending moment appeared for that element. The different total acceleration profiles were then multiplied with the mass matrix to obtain the inertial forces which were set as the load level for load factor $\lambda = 1$. The obtained distributions were then scaled from $\lambda = 0$ until the solution failed to converge. This procedure was conducted on both the full nonlinear model, as well as the one using the ELA iteration scheme.

4 ANALYSIS RESULTS

4.1 THA

The results from the time history analyses show that in general the ELA method was able to capture maximum bending moments in critical sections of the pylon. Table 3 summarizes the maximum forces in selected elements of the pylon, averaged over all seven ground motions for both the initial elastic model and the reduced stiffness model obtained through ELA. The average reduction ratios from the initial stiffness of the elements are also included in the table. The moments are normalized by the bending moment values following the NTHA by using the formula

$$M^* = \frac{M}{M_{fiber}} \tag{2}$$

Element	Ratio	$M^*_{y,initial}$	$M^*_{y,final}$	$M_{y,fiber}$ [MNm]
4101	0.63	1.12	1.06	338
4103	0.80	1.11	1.03	274
4106	0.99	1.10	0.96	187
4112	0.99	1.04	1.21	92
4115	0.82	1.10	1.11	192
4120	1.00	1.04	1.03	53
4501	0.31	1.27	1.03	185
4701	0.35	1.13	1.01	137

Table 3: Summary of average normalized bending moments about the bridges transverse axis.

Figure 3 and 4 plot the displacement and moment response histories of the full nonlinear fiber model, the initial elastic model and the converged model using the ELA for one of the input ground motions. The maximum bending moment response for each model is highlighted in the plot. Figure 5 shows the maximum absolute value of the bending moments at the base of the pylon normalized against the bending moment response of the fiber section model, with the average values across all seven ground motions plotted at the bottom.

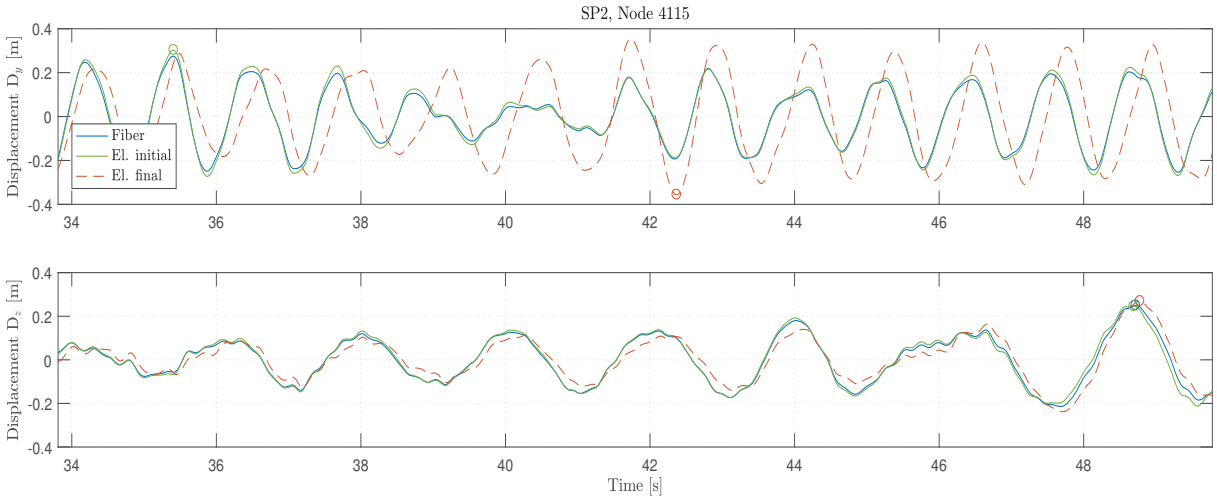

Figure 3: Displacement response history of upper part of pylon.

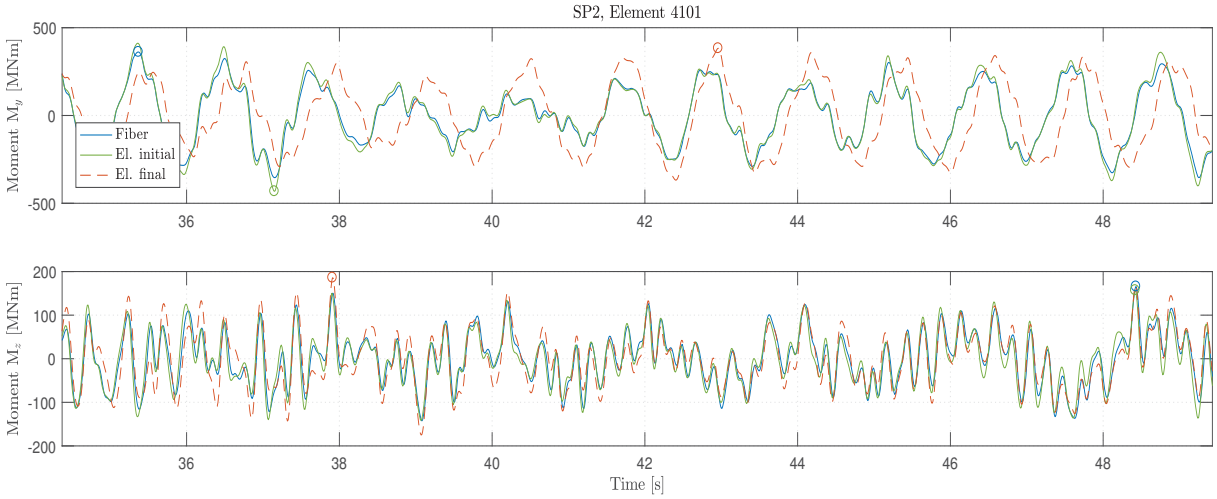

Figure 4: Moment response history in base of pylon.

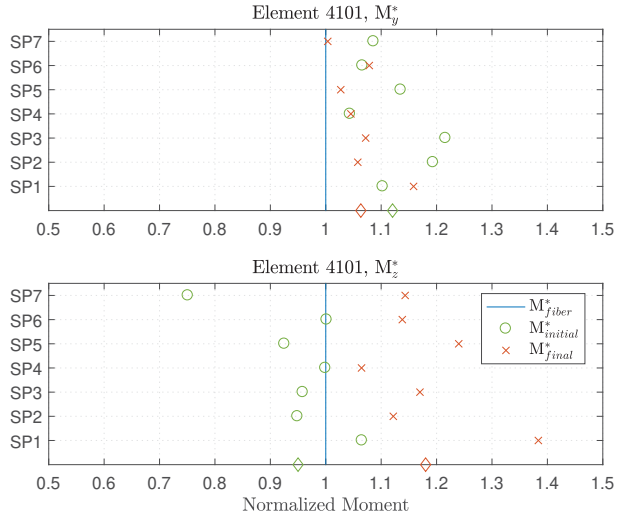

Figure 5: Moment response history of element 4101.

When studying the time histories for the various input ground motions, it is clear that in the ELA performed well in approximating the bending moments in the pylon. From Table 3, the largest deviation between the final iteration of the ELA and the full nonlinear model was 21%, which occurs in element 4112. A possible reason for the deviation in this element is the combination of low bending moment levels and large deflections in this particular area of the pylon. This in turn means that the forces and therefore reduction ratios are largely governed by the stiffness of the remaining elements of the pylon and consequentially second order geometrical effects plays a significant role. This effect can also be seen in the bottom part of Figure 5, where the M_z values appear quite spurious, and are in general larger for the final iteration of the model based on the ELA than the model with initial stiffnesses. This is a general trend in areas with small bending moments and can be attributed to second order geometrical effects.

For the remaining elements listed in the table, the largest deviations were in the range of 1-11%, which from an engineering point of view is acceptable for an approximate method. For the displacement time histories, the model using the ELA was slightly shifted in its response compared to the model with initial stiffnesses and the full nonlinear model. This is is explained

by the fact that the stiffness of the various elements in the ELA model are based on the largest forces throughout the response history. The ELA model also does not include closing of cracks which in sum yields a lower stiffness and therefore larger, phase-shifted displacements.

4.2 Pushover analysis

The pushover analyses conducted in this study served as a foundation for verifying the results from the THAs, as well as a separate examination for comparing the response of structures using the ELA and nonlinear material models. Figure 6 plots the load-displacement pushover curve for the analysis L1, while Figure 7 plots the moment distributions for load factor $\lambda = 1$ and $\lambda = 1.5$ where the latter is the load factor where the model using the ELA failed to converge. Analysis L1 corresponds to the inertial force level and distribution which yields the largest bending moments at the base of the western pylon leg, that is, element 4101. The results for the base and upper part of the pylon are summarized in Table 4.

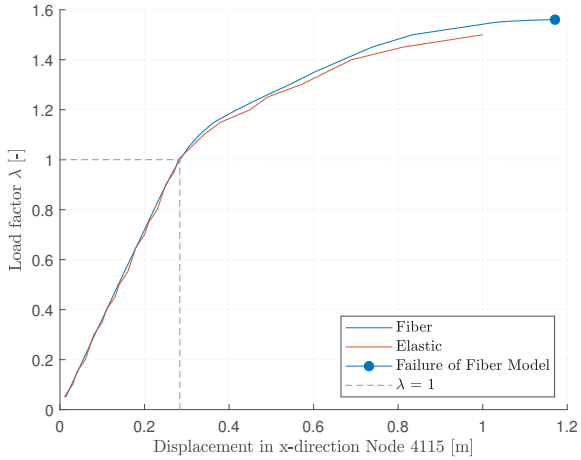

Figure 6: Force-displacement pushover curve for analysis L1.

When transient and cyclic effects are excluded, the pushover analyses shows the ELAs ability of accurately approximating the nonlinear model during static analysis. The various pushover analyses conducted demonstrate that the ELA performed well both up to the load level retrieved from the THAs and beyond. For design purposes, pushover analyses performed on models with the ELA method can be used to predict the location of possible plastic hinges. It can also be implemented to control safety factors for given load levels from transient analyses.

Element	Ratio $\lambda = 1$	$M^*_{\lambda=1}$	Ratio $\lambda = 1.5$	$M^*_{\lambda=1.5}$
4101	0.95	0.99	0.47	1.03
4201	0.95	1.00	0.47	1.04
4115	0.92	1.02	0.47	1.05
4215	0.93	1.01	0.31	1.04

Table 4: Summary of critical element for pushover analysis L1.

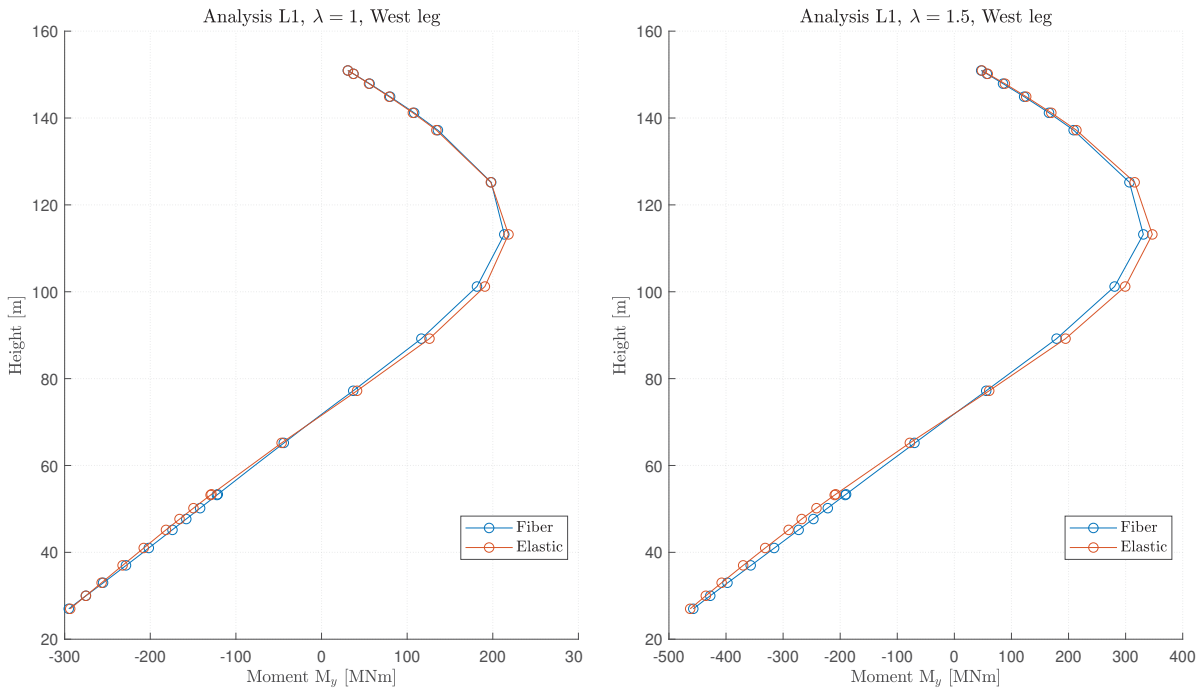

(a) (b)

Figure 7: Moment distribution in the pylon legs for analysis L1.

5 CONCLUSION

The goal of this study has been to assess if the the secant stiffness can provide a reasonable approximation to the nonlinear material behavior of structures. By assessing the forces succeeding ELAs and comparing these to the forces following full NTHAs, several remarks can be made. For the majority of elements the approximation of forces is satisfactory, especially for those enduring large moments during the THA. There are however anomalies where the ELA increases the gap between responses which may be rooted in the shortcomings of the method. Unlike a full NTHA, the ELA is not able to take effects such as cyclic degradation, closing of cracks and dissipation of energy due to cracking of the concrete into consideration. Further, since the stiffness reduction developments occur independent of each other during each iteration, information regarding interaction between elements is lost.The consequence of this is an overall softer structure, with certain unpredictable properties. Rather than using the stiffness values obtained following the ELA, it is proposed to use these as guidelines for creating new ones. By selecting stiffnesses enveloped by the initial and reduced values, more towards the latter, overestimation of stiffness reduction is counteracted. The resulting structure will then inherit a realistic crack distribution. The quality of the nonlinear approximation was confirmed by pushover analyses, where the ELA was capable of accurately producing similar bending moment and deflection patterns as the nonlinear fiber model. When reaching load levels where post-yield capacity was expected, the ELA produced bending moments with slightly higher values in the elements experiencing the largest stiffness reductions. This is due to how the ELA obtains secant stiffnesses for moments close to the section's ultimate capacity.

Overall, the ELA has proven to be a valid alternative to a full nonlinear analysis. The method is also code-compliant as it satisfies the requirements from both Eurocode 8 and the AASHTO Guide Specifications for LRFD Seismic Bridge Design with regards to providing results that are consistent with expected nonlinear material behaviour.

6 ACKNOWLEDGMENTS

This paper is partly based on the MSc thesis of the first two authors in the Department of Structural Engineering at the Norwegian University of Science & Technology (NTNU) [12]. These authors would like to thank Aas-Jakobsen for providing the neccecary resources for preparing this paper, as well as their general support for this study.

REFERENCES

[1] S.E. Barrientos. Earthquakes in Chile. *Geological Society Special Publication*, 01 2007.

[2] J. R. Elliott, E. Hussain, V. Silva, M. Villar-Vega, R. Amey, and G. Rauscher. Contrasting Seismic Risk for Santiago, Chile, from Near-field and Distant Earthquake Sources. In *AGU Fall Meeting Abstracts*, volume 2018, pages G13A–03, December 2018.

[3] RM Bridge. *Connect Edition*. Benteley Systems Incorporated, Exton, Pennsylvania, 2019.

[4] Aas-Jakobsen, SYSTRA, Hyundai Engineering & Construction, and OAS. *Dynamic Impedances and Foundation Input Motions*. Report CHB-SAJ-DGN-DOC-GB-0223, 2018. Not publicly available.

[5] Enrico Spacone, Filip C Filippou, and Fabio F Taucer. Fibre beam–column model for non-linear analysis of r/c frames: Part i. formulation. *Earthquake Engineering & Structural Dynamics*, 25(7):711–725, 1996.

[6] A.K. Chopra. *Dynamics of Structures: Theory and Applications to Earthquake Engineering*. Civil Engineering and Engineering Mechanics Series. Prentice Hall, 2012.

[7] American Association of State Highway, Transportation Officials. Subcommittee on Bridges, and Structures. *AASHTO Guide Specifications for LRFD Seismic Bridge Design*. American Association of State Highway and Transportation Officials, 2011.

[8] Standard Norge. *Eurocode 8: Design of structures for earthquake resistance - Part 1: General rules, seismic action and rules for buildings*. NS-EN 1998-1:2004+A1:2013+NA:2014, 2014.

[9] Frank McKenna, Silvia Mazzoni, Michael H. Scott, and Gregory L. Fenves. Opensees command language manual. *Open System for Earthquake Engineering Simulation*, 2006.

[10] Yassin MH Mohd. Nonlinear analysis of prestressed concrete structures under monotonic and cyclic loads. *PhD Thesis*, 1995.

[11] Filip Filippou, A D'Ambrisi, and A Issa. Effects of reinforcement slip on hysteretic behavior of reinforced concrete frame members. *ACI Structural Journal*, 96, 05 1999.

[12] Tarjei Heen and Kevin W. Kariuki. Investigative study on method for approximating non-linear material behavior in reinforced concrete structures subjected to seismic ground motions. *Master's thesis, Norwegian University of Science & Technology*, 2019.